Volume 59
Number 63
14 August 2023
Pages 9547–9664

ChemComm

Chemical Communications

rsc.li/chemcomm

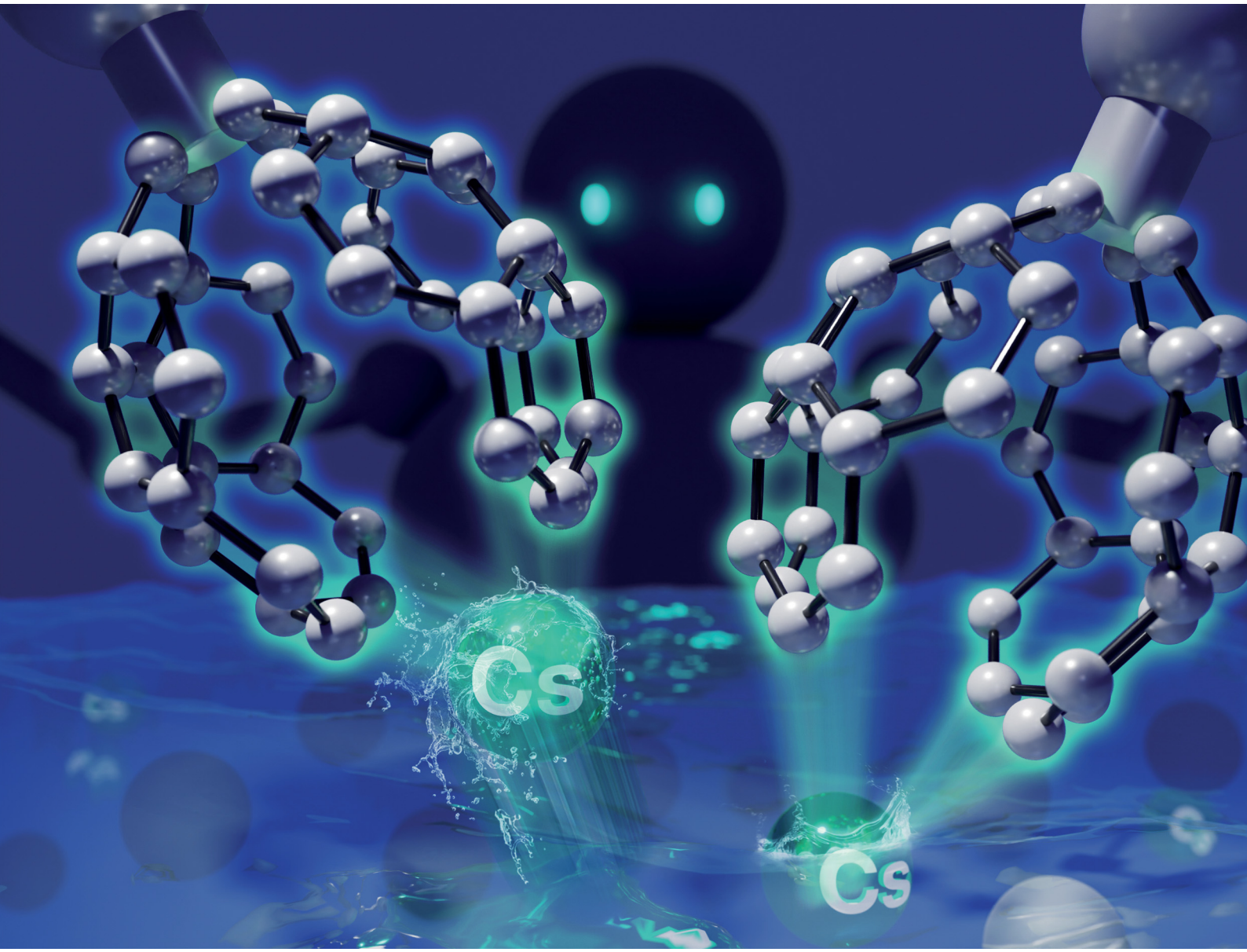

ISSN 1359-7345

ROYAL SOCIETY OF CHEMISTRY

COMMUNICATION

Artur Kasprzak *et al.*

A sumanene-containing magnetic nanoadsorbent for the removal of caesium salts from aqueous solutions

ChemComm

COMMUNICATION

View Article Online
View Journal | View Issue

Cite this: *Chem. Commun.*, 2023, 59, 9591

Received 2nd June 2023,
Accepted 6th July 2023

DOI: 10.1039/d3cc02657d

rsc.li/chemcomm

A sumanene-containing magnetic nanoadsorbent for the removal of caesium salts from aqueous solutions†

Artur Kasprzak, *[a] Magdalena Matczuk [b] and Hidehiro Sakurai [cd]

Sumanene was covalently immobilised onto the surface of cobalt nanomagnets to obtain a magnetic nanoadsorbent. This nanoadsorbent was specifically designed to efficiently and selectively remove caesium (Cs) salts from aqueous solutions. The nanoadsorbent's application potential was evidenced by the removal of Cs from model aqueous solutions, simulating the concentrations of radioactive ^{137}Cs in the environment. Additionally, Cs was effectively removed from aqueous wastes generated by routine chemical processes, including those used in drug synthesis.

The removal of caesium (Cs) salts from aqueous wastes is important from the viewpoint of human health and the protection of the natural environment. Cs contamination originates not only from organic syntheses wastes, where Cs salts like caesium fluoride (CsF) or caesium carbonate are commonly employed but also from the presence of the most dangerous radioactive ^{137}Cs. Over the years, the major source of toxic ^{137}Cs was the nuclear plant disasters, especially the Fukushima-Daiichi nuclear plant disaster in 2011, resulting in the uncontrolled release of significant amounts of radioactive ^{137}Cs into groundwater and seawater.[1–3] These incidents influenced the development of materials for removing Cs salts from liquid samples. The reported adsorbents primarily consist of mineral adsorbents like zeolites[4,5] or graphene-family materials.[5,6] However, these adsorbents featured low Cs-selectivity, leading to the unwanted, competitive removal of other salts present in the sample, such as sodium, potassium, or magnesium salts.

Sumanene (**1**; Fig. 1), firstly synthesised in 2003,[7,8] is the polyaromatic subunit of fullerene C_{60}, belonging to the group of the so-called *buckybowls*. The bowl shape of sumanene is a significant factor influencing interest in this molecule. This unique feature implies interesting properties of sumanene derivatives[9–11] and is a powerful tool in synthesising highly organised structures.[12,13] Consequently, sumanene and *buckybowls*, in general, are extensively discussed in terms of their applications. However, the reports on the practical applications of sumanene remain limited. Recently, from 2019 to 2023, we reported on the application of sumanene–ferrocene conjugates as highly selective and sensitive voltammetric sensors[14–17] for detection of caesium cations (Cs^+). The mechanism of action involved cation–π interactions and the perfect size match between the concave side of the sumanene bowl and the van der Waals radius of Cs^+.[18–20] Inspired by these studies, we further investigated the potential application of the sumanene molecule. In pursuit of discovering new practical applications of sumanene, we intended the design a new class of adsorbent dedicated to removing Cs salts from aqueous solutions. Combining the chemistries of sumanene and magnetic nanomaterials seemed particularly appealing. Magnetic nanomaterials show promise for various applications, including catalysis[21–23] or adsorbent technologies.[24,25] One of their key features is their ease of separation from the liquid phase using an external magnetic field (a permanent magnet) without the need for centrifugation or filtration. In this work, we present the design and synthesis of surface-functionalised cobalt nanomagnets with sumanene. These magnetic nanomaterials serve as the first magnetic nano-adsorbent **11** containing buckybowl structures, specifically designed for the selective removal of Cs salts from aqueous solutions.

The synthesis of the target magnetic nanoadsorbent **11** involved three steps, utilising commercially available carbon-coated cobalt nanomagnets[26] **6** (Fig. 1). Full experimental details can be found in ESI,† Section S1. In brief, firstly, carboxylic functionalities were introduced onto the surface of

[a] *Chair of Organic Chemistry, Faculty of Chemistry, Warsaw University of Technology, Warsaw 00-664, Poland. E-mail: artur.kasprzak@pw.edu.pl*
[b] *Chair of Analytical Chemistry, Faculty of Chemistry, Warsaw University of Technology, Warsaw 00-664, Poland*
[c] *Division of Applied Chemistry, Graduate School of Engineering, Osaka University, Suita 565-0871, Osaka, Japan*
[d] *Innovative Catalysis Science Division, Institute for Open and Transdisciplinary Research Initiatives (ICSOTRI), Osaka University, Suita 565-0871, Osaka, Japan*

† Electronic supplementary information (ESI) available: Experimental section, characterization data, adsorption experiments data. See DOI: https://doi.org/10.1039/d3cc02657d

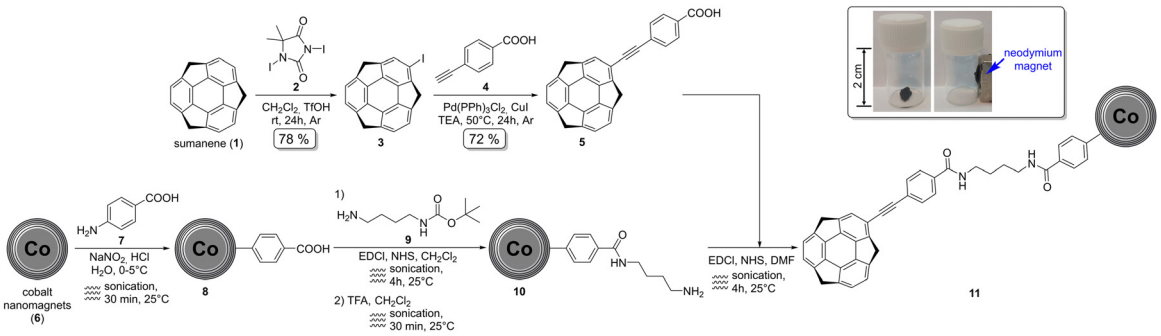

Fig. 1 Synthesis of the target magnetic nanoadsorbent **11**. The frame presents the response of **11** (50 mg) to a permanent magnet.

cobalt nanomagnets **6** using the diazotisation reaction with 4-aminobenzoic acid **7**. As-obtained material **8** was functionalised to primary amino groups in two steps, *i.e.*, by means of the carbodiimide-mediated amidation-type reaction with **9** followed by the Boc-deprotection reaction under acidic conditions. The target magnetic nanoadsorbent **11** was synthesised by means of the amidation-type reaction from material **10** and sumanene derivative **5**, which was obtained in good yield employing the Sonogashira cross-coupling between 2-iodosumanene **3** and 4-ethynylbenzoic acid **4**.

Confirmation of successful derivatisation of sumanene **1** to compound **5** was achieved through nuclear magnetic resonance spectroscopy and high-resolution mass spectrometry. Photophysical properties of compound **5** were investigated using UV-vis and emission spectroscopies (data available in ESI,† Section S2).

To comprehensively analyse the target magnetic nanoadsorbent **11**, various spectroscopic and materials characterisation techniques were employed. These included Fourier-transform infrared spectroscopy (FT-IR), X-ray photoelectron spectroscopy, Raman spectroscopy, powder X-ray diffraction, thermogravimetric analysis (TGA), transmission electron microscopy (TEM) with energy-dispersive X-ray spectroscopy (EDS) using the high-angle annular dark-field (HAADF) technique, scanning electron microscopy (SEM), and elemental analysis. The detailed characterisation can be found in ESI,† Section S2. The analyses confirmed the successful introduction of the desired moieties on the nanomaterial's surface, such as the presence of amide-I bands at *ca.* 1645 cm^{-1} in the FT-IR spectra (Fig. 2b). Furthermore, the presence of each element (C, H, N, O Co) in resultant material **11** was confirmed. The content of sumanene moieties in the resultant material is *ca.* 9 wt% (estimated from TGA analysis, see data in ESI,† Section S2). Notably, microscopic analyses revealed the unharmed core–shell structure of the resultant cobalt nanomagnets-containing material **11** and the presence of a non-uniform thin layer covering the carbon surface of nanoparticles, attributed to the introduced moieties (Fig. 2c; for representative TEM and SEM images, see data in ESI,† Section S2). EDS–HAADF–TEM analyses also indicated relatively homogeneous surface modification of the carbon layer of the nanomagnets (for details, see ESI,† Section S2). The magnetic nanoadsorbent **11** featured promising magnetic properties, as illustrated in Fig. 1. The material could be easily dispersed in water by simple shaking

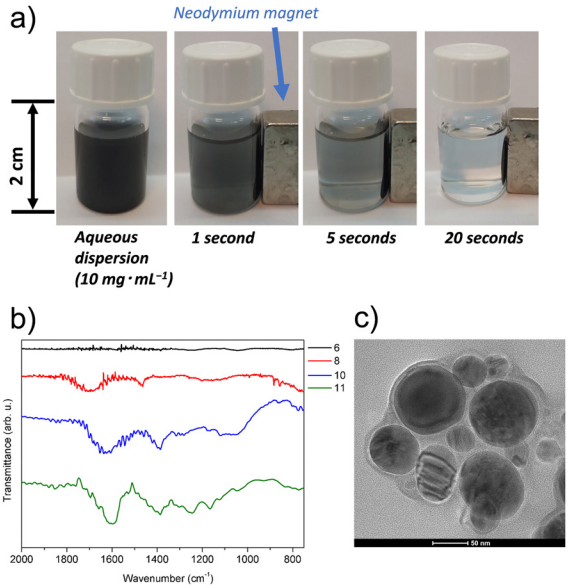

Fig. 2 (a) Response of the aqueous dispersion of magnetic nanoadsorbent **11** to a permanent magnet; (b) FT-IR spectra of materials **6**, **8**, **10**, **11**; (c) TEM image of magnetic nanoadsorbent **11**.

and features a fast and effective response to the external magnetic field in dispersion (see Fig. 2a).

The adsorption properties of magnetic nanoadsorbent **11** towards Cs were investigated using aqueous solutions of caesium chloride (CsCl), which served as a representative Cs salt simulating the concentrations of radioactive ^{137}Cs in the environment. The concentrations of Cs, Na, and K in the samples were determined using inductively coupled plasma tandem mass spectrometry (ICP-MS/MS). Each adsorption experiment was repeated three times to ensure repeatability. After each adsorption trial, the magnetic properties of magnetic nanoadsorbent **11** allowed for easy and simple separation from the solution using a permanent magnet.

The adsorption experiments demonstrated the effective removal of Cs by magnetic nanoadsorbent **11** (Fig. 3a). Notably, SEM-EDS experiment confirmed the presence of adsorbed Cs on the surface of the magnetic nanoadsorbent **11** (the SEM image and EDS spectrum is provided in ESI,† Section S3). The adsorption process exhibited characteristics consistent with the Langmuir adsorption model,[27] suggesting the formation of a

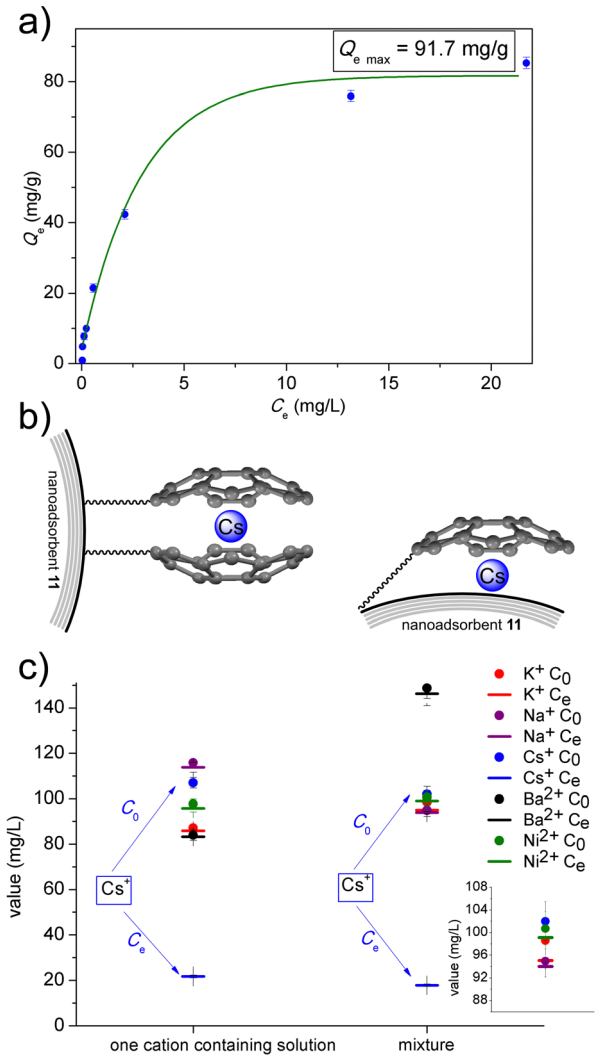

Fig. 3 (a) Adsorption isotherm of Cs adsorption with the magnetic nanoadsorbent **11** (the Langmuir model fitting is also presented); (b) graphical representation of the possible binding modes of Cs; (c) graphical presentation of the results of selectivity tests.

monolayer on the surface (data available in ESI,† Section S3). Using the Langmuir model, the maximum adsorption capacity (Q_{emax}) and Langmuir constant (K_L) for the designed magnetic nanoadsorbent **11** were estimated to be 91.7 mg g^{-1} and 5.9×10^{-4} L g^{-1}, respectively (details in ESI,† Section S3). In comparison, the Cs adsorption test using native cobalt nanomagnets **6** (surface area of native cobalt nanomagnets **6** is >15 m^2 g^{-1} according to work[24] and Merck, product no. 697745) revealed a Q_{emax} value of approximately 4.4 mg g^{-1} (data in ESI,† Section S3). This value is consistent with literature data on the removal of other metal cations using similar carbon-encapsulated magnetic nanoparticles,[25] and significantly lower than that of magnetic nanoadsorbent **11**. This indicates the essential role of sumanene moieties on the surface of magnetic nanoadsorbent **11** in providing beneficial Cs adsorption properties. Zeta potential analyses revealed that the surface zeta potential of cobalt nanomagnets **6** (-9.0 ± 0.6 mV, in H_2O) is *ca* 2-fold higher in comparison to the respective value for the nanoadsorbent **11** (-18.7 ± 1.0 mV). Materials comprising cobalt nanomagnets **6** are also highly magnetic, thus, their particles spontaneously agglomerate in dispersion. Interestingly, dynamic light scattering (DLS) measurements revealted the lower mean hydrodynamic diameter or particles of **11** in comparison to **6** (see size distribution histograms in ESI,† Section S3). This finding suggested that the designed functionalization method might limit the spontaneous aggregation of particles, thus, might influenced the improved dispersion stability. These findings form surface zeta potential and DLS measurements further supported the improved adsorption performance of **11** in comparison to **6**.

Considering the estimated Q_{emax} value for magnetic nanoadsorbent **11** (91.7 mg g^{-1}) and the mass content of sumanene moieties in the resultant material (*ca.* 9 wt%), it can be concluded that the mass ratio of Cs to sumanene is *ca.* 1 : 1, corresponding to a molar ratio of approximately 1 : 2. This suggests that the adsorption process may involve the formation of sandwich-type complexes between Cs and sumanene, as well as the potential involvement of the carbon layer of nanoparticles in the studied adsorption phenomena (see graphical representation of possible binding modes in Fig. 3b). Notably, the Cs adsorbption tests with **11** were also supported by the spectrofluorimetric investigation of sandwich-type complexes between sumanene (**1**) and caesium cations, which further supported the crucial role of sumanene moiety in **11** toward providing Cs binding property of the nanoadsorbent. (Apparent binding constant of 6.6×10^5 M^{-2} was concluded for this system, see data and discussion in ESI,† Section S7).

The Q_{emax} value obtained for magnetic nanoadsorbent **11** demonstrates its superior adsorption capacity compared to previously reported adsorbents, including mineral adsorbents, graphene family materials, metal–organic frameworks (MOFs), crown ether or calixarene-containing materials, and iron oxide-based magnetic adsorbents (data available in ESI,† Section S3). Additionally, the magnetic nanoadsorbent **11** offers the advantage of easy magnetic separation from the liquid phase, making its removal from the treated aqueous solution the most facile and the fastest among all reported Cs adsorbents. Kinetic analyses revealed the most effective contact time to be 30 min (data in ESI,† Section S3).

Our experiments also revealed the possibility of reusing magnetic nanoadsorbent **11**. After the adsorption process and magnetic separation, **11** could be easily recovered by washing with a small volume of water (see details in ESI,† Section S3). The magnetic nanoadsorbent **11** demonstrated reusability for at least four adsorption cycles. The results of each adsorption cycle were highly consistent, indicating the effectiveness of the washing process during the recovery stage. Regeneration of magnetic nanoadsorbent **11** after the adsorption process was also supported with the FT-IR spectroscopy, TEM microscopy and elemental analysis (see details in ESI,† Section S3). In particular, these analyses supported the elemental composition of the regenerated **11** sample, as well as confirmed no significant morphological differences between the samples of **11** before adsorption and after the regeneration process.

The high selectivity of magnetic nanoadsorbent **11** for Cs removal can be anticipated[14–17] due to the presence of sumanene

moieties on its surface. To investigate this selectivity, similar adsorption experiments were conducted using sodium (Na), potassium (K), barium (Ba), and nickel (Ni) salts, which are representative interferents or toxins, which might found in the environment, groundwater, and drinking water (Fig. 3c). The results demonstrated the high selectivity of magnetic nanoadsorbent **11** for Cs removal, even in the presence of interferents (see complete data in ESI,† Section S3). No interfering effect of Ba is essential, since Ba^{2+} features similar van der Waals radius as Cs^{+}. This finding supports the hypothesis that the site-selective cation-π interactions between Cs^{+} and concave site of sumanene bowls[14–17] shall play a vital role in the recognition phenomenon.

The application potential of magnetic nanoadsorbent **11** was further elucidated by utilizing it for the removal of Cs-containing aqueous wastes generated during the synthesis of (*R*,*E*)-*N*-(2,5-difluorobenzylidene)-2-methylpropane-2-sulfinamide **14** from (*R*)-2-methylpropane-2-sulfinamide **13** and 2,5-difluorobenzaldehyde **12** (for data and detailed information, refer to ESI,† Section S4). Compound **14** serves as a starting material in the synthesis of *larotrectinib*®, an anticancer drug recently approved by the FDA.[28] The production of caesium-containing aqueous wastes in this synthesis is a result of the use of caesium carbonate (Cs_2CO_3). Our experiments demonstrated that the designed magnetic nanoadsorbent **11** effectively removes Cs_2CO_3 from the aqueous wastes generated in this process. Importantly, the effective action of magnetic nanoadsorbent **11** was confirmed by the detection of Cs on the surface of material **11** after the adsorption process. Note that this finding is constistent with the SEM-EDS experiment on model tests of CsCl adsorption with **11**, in which the presence of adsorbed Cs on the surface of **11** was confirmed.

To further demonstrate the general application potential of magnetic nanoadsorbent **11**, we focused on using this material for the removal of toxic caesium salts from aqueous wastes generated in commonly performed processes in organic chemistry laboratories. For this purpose, we selected the desilylation reaction, where caesium salts, such as CsF, are commonly used as desilylating agents.[29,30] In our experiments, the CsF-containing aqueous wastes were generated in a representative CsF-mediated desilylation of (4-bromophenoxy)(*tert*-butyl)dimethylsilane **15** to 4-bromophenol **16** (for data and detailed information, refer to ESI,† Section S5). After treating the CsF-containing aqueous waste with the designed magnetic nanoadsorbent **11**, we observed practically complete removal of caesium. This conclusion was further supported by detecting the presence of adsorbed Cs on the surface of magnetic nanoadsorbent **11**.

In summary, we have presented the design and synthesis of a novel magnetic nanoadsorbent **11**, incorporating sumanene for the efficient and selective removal of toxic Cs salts from aqueous solutions. The nanoadsorbent exhibited a high maximum adsorption capacity (Q_{emax} = 91.7 mg g^{-1}), easy magnetic separation, selectivity for Cs removal, and the potential for reusability. The effectiveness of the nanoadsorbent was demonstrated in the removal of Cs salts simulating radioactive ^{137}Cs concentrations in the environment, as well as in the treatment of aqueous wastes generated (i) in the desilylation reaction, as the representative routine chemical process in organic chemistry laboratories, and (ii) in the process crucial in the pharmaceutical industry, namely the synthesis of starting material for *larotrectinib*® drug. This work paves the way for future research on practical applications of sumanene derivatives and *buckybowls* in general and represents a significant advancement in Cs salt removal technologies.

This research was funded by POB Technologie Materiałowe of Warsaw University of Technology through the Excellence Initiative: Research University (IDUB) programme, agreement no. 1820/335/Z01/POB5/2021 (A. K.), and JSPS KAKENHI grant no. JP19H00912 and JP21H05233 (H.S.).

Conflicts of interest

There are no conflicts to declare.

Notes and references

1 H. Kaeriyama, *Fish. Oceanogr.*, 2017, **26**, 99–113.
2 T. Mizuno and H. Kubo, *Sci. Rep.*, 2013, **3**, 1742.
3 T. J. Yasunari, A. Stohl, R. S. Hayano, J. F. Burkhart, S. Eckhardt and T. Yasunari, *Proc. Natl. Acad. Sci. U. S. A.*, 2011, **108**, 19530–19534.
4 S. Kwon, Y. Kim and Y. Roh, *Sci. Rep.*, 2021, **11**, 15362.
5 X. Liu, G.-R. Chen, D.-J. Lee, T. Kawamoto, H. Tanaka, M.-L. Chen and Y.-K. Luo, *Bioresour. Technol.*, 2014, **160**, 142–149.
6 P. Kaewmee, J. Manyam, P. Opaprakasit, G. T. Truc Le, N. Chanlek and P. Sreearunothai, *RSC Adv.*, 2017, **7**, 38747–38756.
7 H. Sakurai, T. Daiko and T. Hirao, *Science*, 2003, **301**, 1878.
8 H. Sakurai, *Bull. Chem. Soc. Jpn.*, 2021, **94**, 1579–1587.
9 T. Amaya and T. Hirao, *Chem. Rec.*, 2015, **15**, 310–321.
10 T. Amaya and T. Hirao, *Chem. Commun.*, 2011, **47**, 10524.
11 M. Saito, H. Shinokubo and H. Sakurai, *Mater. Chem. Front.*, 2018, **2**, 635–661.
12 Y. Yakiyama, T. Hasegawa and H. Sakurai, *J. Am. Chem. Soc.*, 2019, **141**, 18099–18103.
13 I. Hisaki, H. Toda, H. Sato, N. Tohnai and H. Sakurai, *Angew. Chem., Int. Ed.*, 2017, **56**, 15294–15298.
14 A. Kasprzak and H. Sakurai, *Dalton Trans.*, 2019, **48**, 17147–17152.
15 A. Kasprzak, A. Kowalczyk, A. Jagielska, B. Wagner, A. M. Nowicka and H. Sakurai, *Dalton Trans.*, 2020, **49**, 9965–9971.
16 J. S. Cyniak, Ł. Kocobolska, N. Bojdecka, A. Gajda-Walczak, A. Kowalczyk, B. Wagner, A. M. Nowicka, H. Sakurai and A. Kasprzak, *Dalton Trans.*, 2023, **52**, 3137–3147.
17 A. Kasprzak, A. Gajda-Walczak, A. Kowalczyk, B. Wagner, A. M. Nowicka, M. Nishimoto, M. Koszytkowska-Stawińska and H. Sakurai, *J. Org. Chem.*, 2023, **88**, 4199–4208.
18 S. N. Spisak, Z. Wei, A. Y. Rogachev, T. Amaya, T. Hirao and M. A. Petrukhina, *Angew. Chem., Int. Ed.*, 2017, **56**, 2582–2587.
19 U. D. Priyakumar and G. N. Sastry, *Tetrahedron Lett.*, 2003, **44**, 6043–6046.
20 D. Vijay, H. Sakurai, V. Subramanian and G. N. Sastry, *Phys. Chem. Chem. Phys.*, 2012, **14**, 3057.
21 A. Schätz, T. R. Long, R. N. Grass, W. J. Stark, P. R. Hanson and O. Reiser, *Adv. Funct. Mater.*, 2010, **20**, 4323–4328.
22 C. G. Tan and R. N. Grass, *Chem. Commun.*, 2008, 4297.
23 A. Kasprzak, M. Bystrzejewski and M. Poplawska, *Org. Process Res. Dev.*, 2019, **23**, 409–415.
24 R. Fuhrer, I. K. Herrmann, E. K. Athanassiou, R. N. Grass and W. J. Stark, *Langmuir*, 2011, **27**, 1924–1929.
25 P. Strachowski, W. Kaszuwara and M. Bystrzejewski, *New J. Chem.*, 2017, **41**, 12617–12630.
26 R. N. Grass, E. K. Athanassiou and W. J. Stark, *Angew. Chem., Int. Ed.*, 2007, **46**, 4909–4912.
27 H. Swenson and N. P. Stadie, *Langmuir*, 2019, **35**, 5409–5426.
28 H. Mei, J. Han, S. Fustero, M. Medio-Simon, D. M. Sedgwick, C. Santi, R. Ruzziconi and V. A. Soloshonok, *Chem. – Eur. J.*, 2019, **25**, 11797–11819.
29 M. Fiorenza, A. Mordini, S. Papaleo, S. Pastorelli and A. Ricci, *Tetrahedron Lett.*, 1985, **26**, 787–788.
30 J. H. Clark, *Chem. Rev.*, 1980, **80**, 429–452.